

UCLA

UCLA Previously Published Works

Title

A Translational Porcine Model for Human Cell-Based Therapies in the Treatment of Posttraumatic Osteoarthritis After Anterior Cruciate Ligament Injury.

Permalink

<https://escholarship.org/uc/item/2b46x4br>

Journal

American Journal of Sports Medicine, 48(12)

Authors

Kremen, Thomas
Stefanovic, Tina
Tawackoli, Wafa
[et al.](#)

Publication Date

2020-10-01

DOI

10.1177/0363546520952353

Peer reviewed



Published in final edited form as:

Am J Sports Med. 2020 October ; 48(12): 3002–3012. doi:10.1177/0363546520952353.

A Translational Porcine Model for Human Cell–Based Therapies in the Treatment of Posttraumatic Osteoarthritis After Anterior Cruciate Ligament Injury

Thomas J. Kremen Jr, MD^{*,†}, Tina Stefanovic, BS^{‡,§}, Wafa Tawackoli, PhD^{‡,§,||,¶,#}, Khosrowdad Salehi, BS^{‡,§}, Pablo Avalos, MD[§], Derek Reichel, PhD^{||,#,**}, J. Manual Perez, PhD^{||,#,**}, Juliane D. Glaeser, PhD^{‡,§}, Dmitriy Sheyn, PhD^{*,‡,§,||,¶,#,††}, Investigation performed at Board of Governors Regenerative Medicine Institute, Cedars-Sinai Medical Center, Los Angeles, California, USA

[†]Department of Orthopaedic Surgery, David Geffen School of Medicine at UCLA, Los Angeles, California, USA.

[‡]Orthopaedic Stem Cell Research Laboratory, Cedars-Sinai Medical Center, Los Angeles, California, USA.

[§]Board of Governors Regenerative Medicine Institute, Cedars-Sinai Medical Center, Los Angeles, California, USA.

^{||}Biomedical Imaging Research Institute, Cedars-Sinai Medical Center, Los Angeles, California, USA.

[¶]Department of Surgery, Cedars-Sinai Medical Center, Los Angeles, California, USA.

[#]Department of Biomedical Sciences, Cedars-Sinai Medical Center, Los Angeles, California, USA.

^{**}Department of Neurosurgery, Cedars-Sinai Medical Center, Los Angeles, California, USA.

^{††}Department of Orthopedics, Cedars-Sinai Medical Center, Los Angeles, California, USA.

Abstract

Background: There is a high incidence of posttraumatic osteoarthritis (PTOA) after anterior cruciate ligament (ACL) injury, and these injuries represent an enormous health care economic burden. In an effort to address this unmet clinical need, there has been increasing interest in cell-based therapies.

Purpose: To establish a translational large animal model of PTOA and demonstrate the feasibility of intra-articular human cell–based interventions.

Study Design: Descriptive laboratory study.

*Address correspondence to Thomas J. Kremen Jr, MD, Department of Orthopaedic Surgery, David Geffen School of Medicine at UCLA, 1225 15th Street, Suite 2100, Santa Monica, CA 90404, USA (tjkremen@mednet.ucla.edu) (Twitter: @ThomasKremenMD); or Dmitriy Sheyn, PhD, Cedars-Sinai Medical Center, 127 S. San Vicente Blvd, AHSP A8308, Los Angeles, CA 90048, USA (Dmitriy.Sheyn@csmc.edu) (Twitter: @Sheynlab).

One or more of the authors has declared the following potential conflict of interest

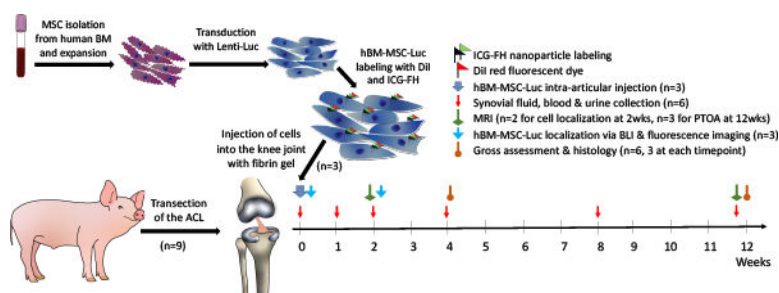
Methods: Nine Yucatan mini-pigs underwent unilateral ACL transection and were monitored for up to 12 weeks after injury. Interleukin 1 beta (IL-1 β) levels and collagen breakdown were evaluated longitudinally using enzyme-linked immunosorbent assays of synovial fluid, serum, and urine. Animals were euthanized at 4 weeks (n = 3) or 12 weeks (n = 3) after injury, and injured and uninjured limbs underwent magnetic resonance imaging (MRI) and histologic analysis. At 2 days after ACL injury, an additional 3 animals received an intra-articular injection of 10⁷ human bone marrow–derived mesenchymal stem cells (hBM-MSCs) combined with a fibrin carrier. These cells were labeled with the luciferase reporter gene (hBM-MSCs-Luc) as well as fluorescent markers and intracellular iron nanoparticles. These animals were euthanized on day 0 (n = 1) or day 14 (n = 2) after injection. hBM-MSC-Luc viability and localization were assessed using ex vivo bioluminescence imaging, fluorescence imaging, and MRI.

Results: PTOA was detected as early as 4 weeks after injury. At 12 weeks after injury, osteoarthritis could be detected grossly as well as on histologic analysis. Synovial fluid analysis showed elevation of IL-1 β shortly after ACL injury, with subsequent resolution by 2 weeks after injury. Collagen type II protein fragments were elevated in the synovial fluid and serum after injury. hBM-MSCs-Luc were detected immediately after injection and at 2 weeks after injection using fluorescence imaging, MRI, and bioluminescence imaging.

Conclusion: This study demonstrates the feasibility of reproducing the chondral changes, intra-articular cytokine alterations, and body fluid biomarker findings consistent with PTOA after ACL injury in a large animal model. Furthermore, we have demonstrated the ability of hBM-MSCs to survive and express transgene within the knee joint of porcine hosts without immunosuppression for at least 2 weeks.

Clinical Relevance: This model holds great potential to significantly contribute to investigations focused on the development of cell-based therapies for human ACL injury–associated PTOA in the future (see Appendix Figure A1, available online).

Graphical Abstract



Keywords

biology of cartilage; knee articular cartilage; ACL; stem cell therapy; posttraumatic osteoarthritis

Anterior cruciate ligament (ACL) injury is one of the most common soft tissue injuries to the knee. It is highly prevalent in patients aged 15 to 45 years, affecting 1 of 1750 people in this age group, with most patients being <30 years of age.¹⁸ It has been estimated that an ACL rupture ages the knee by 30 years.^{14,34} The incidence of posttraumatic osteoarthritis

(PTOA) has been reported to be as high as 87%¹⁴; however, on average, 50% of individuals with an ACL injury will develop radiographic osteoarthritis (OA) approximately 10 to 20 years after ACL or meniscal injury.²⁶ To date, there is no effective intervention, including the restoration of mechanical stability via ACL reconstruction, to prevent PTOA associated with ACL injury.²⁸ In addition to the clinical morbidity associated with PTOA, the high incidence of OA in this relatively young population presents significant long-term financial challenges to health care systems. In fact, it has been estimated that innovations in the treatment of ACL injuries that result in a decreased relative risk of radiographic knee OA by just one-fourth of its current value would save the United States \$460 million annually.³⁵ Thus, PTOA after ACL injury represents an enormous unmet clinical need in our society and, as a result, is a highly active area of research worldwide.

Translational animal models of this human disease are fundamental to this line of research. Although the possibility of genetic manipulations for mechanistic *in vivo* studies is a distinct advantage of murine animal models, rodent models of cartilage disease often lack a high degree of translational potential owing to these animals' intrinsic regenerative potential as well as the small scale and low physiologic demand of their anatomy.¹⁰ As a result of the larger-caliber knee joint and the high prevalence of naturally occurring ACL injuries in dogs, the canine ACL injury model gained popularity as a large animal translational model of degenerative joint disease. One reason for this was the increased posterior tibial slope ($\sim 24^\circ$)⁵ of the canine tibia relative to humans, which causes abnormal biomechanical properties likely contributing to accelerated progression of degenerative joint disease. The canine model does, however, have 2 significant limitations: cartilage thickness significantly less than that of humans and ethical considerations.¹⁰ As a result, protocols proposing canine animal models fall under greater Institutional Animal Care and Use Committee scrutiny than other similarly sized animals.¹⁰ As an alternative to canine models of ACL injury, porcine models offer several advantages. The large-caliber, translationally relevant porcine knee is also noted to have an increased posterior lateral tibial slope ($\sim 35^\circ$).²³ Moreover, sex-specific anatomic differences among porcine knees have been validated to be comparable with sex-specific knee findings among humans.²³ In addition, the cartilage of a porcine knee is thicker than that of canine knees and thus more closely resembles the thickness of human cartilage.¹⁰ This feature allows for the study of partial-thickness cartilage loss, which is a finding commonly observed with the development of human PTOA.¹⁰ As a result, porcine models constitute a highly translational model for the study of PTOA after ACL injury.

The development of late-phase OA in the injured joint is thought to be the result of inflammation that is initiated in response to an injury combined with the long-term changes in dynamic joint loading.³³ Interleukin 1 (IL-1) is the dominant cytokine in the joint that appears to trigger the development of early OA, and overexpression of IL-1 alone can initiate the development of arthritis *in vivo*.²⁸ Furthermore, IL-1 beta (IL-1 β) levels in the human knee have been shown to increase acutely after ACL injury and then normalize to physiologic levels about 2 weeks after injury.⁷ Thus, monitoring IL-1 β levels after ACL injury is an essential component of evaluating the physiologic state of an injured knee joint.

At a time when biologic therapies of musculoskeletal injuries are expanding exponentially, cell-based therapeutic interventions have garnered a considerable amount of attention. These cell-based therapies include minimally manipulated cells that are already being implemented clinically, as well as transgenic cells being used investigatively as drug delivery vehicles. In either case, the translational potential of cell-based therapies holds great promise.

Therapeutic cells can be labeled using a variety of techniques, including fluorescent dyes, ^{11,36,42,43} reporter genes,²⁷ and Food and Drug Administration (FDA)–approved iron oxide nanoparticles.^{27,54} It is also possible to combine these approaches, as has been shown in the detection of labeled cancer cells with an FDA-approved iron oxide nano-particle, Feraheme (FH; ferumoxytol), combined with the near-infrared fluorescent dye indocyanine green (ICG). On the basis of these previous observations, we speculated that the labeling of human mesenchymal stem cells (MSCs) with FH(ICG) nanoparticles, the fluorescent dye DiI, and the luciferase reporter gene (Luc) would allow for the detection and monitoring of therapeutic cells in a large animal model using magnetic resonance imaging (MRI), fluorescence imaging, and bioluminescence imaging.

In this investigation, we describe a novel technique for the percutaneous intra-articular delivery of transgenic human MSCs in the setting of a porcine model of PTOA after ACL injury. We hypothesized that transection of the ACL in porcine knees would lead to degenerative changes analogous to those observed in human PTOA several years after ACL injury. Furthermore, we hypothesized that xenogeneic MSCs would not only be viable but also express transgenic proteins within the injured knee joint for at least 2 weeks after percutaneous implantation (Table 1).

METHODS

Study Design

The aim of this study is to develop a valuable model of PTOA in large animals to study cell therapy–based interventions shortly after an ACL injury. The ACL injury was simulated by transection of the ACL in the right knee of 9 mini-pigs using an open surgical approach. Animals in group 1 (n = 6) were monitored for OA formation by sampling body fluids (synovial fluid from the injured and contralateral uninjured knee joints, venous blood, and urine) for OA biomarkers on weeks 1, 2, 4, 8, and 12 after ACL injury. IL-1 β levels were also measured in the synovial fluid, serum, and urine using an enzyme-linked immunosorbent assay (ELISA). Collagen breakdown was determined using an ELISA for collagen type II fragments in the serum, synovial fluids, and urine of study animals. Animals were euthanized at 4 weeks (n = 3) or 12 weeks (n = 3) after injury, and their injured and uninjured limbs were harvested for MRI, followed by gross and histologic analysis of the knee joints. To estimate the survival of xenogeneic human cells, human bone marrow (hBM)–MSC-Luc constructs were labeled with multiple cell-tracking techniques, resuspended in fibrin gel, and percutaneously injected under fluoroscopic guidance into the injured knee joint of a second group of animals (group 2; n = 3) 2 days after the ACL injury. One group of 1 animal was sacrificed on day 0 after the injection to assess the ability of the bioluminescence imaging system to detect viable cells inside a porcine knee. The remaining animals (n = 2) were euthanized 14 days after cell delivery (16 days after ACL injury) for

assessment of cell viability and localization within the knee joint using bioluminescence imaging, fluorescence imaging, and MRI.

ACL Injury Model

All animal procedures were approved by the Cedars-Sinai Medical Center Institutional Animal Care and Use Committee (007984) and conducted in accordance with Animal Research: Reporting of In Vivo Experiments (ARRIVE) guidelines.²⁴ Nine 6- to 8-month-old female Yucatan mini-pigs (S&S Farm) weighing 30 to 35 kg at the time of surgery were included in this study. Animals were housed in group (pen with an average size of 3–5 m² equipped with environmental enrichment) for a minimum of 1 week before enrollment in the study. The comparative medicine husbandry staff provided food twice daily and water at all times.

Animals were fasted for approximately 18 hours before the surgical procedure. Each mini-pig was sedated with intramuscular acepromazine (0.25 mg/kg), ketamine (20 mg/kg), and atropine (0.02–0.05 mg/kg), followed by intravenous propofol (2 mg/kg). Animals were intubated, and anesthesia was maintained using 1.0% to 3.5% inhaled isoflurane for the duration of the surgical procedure. The animals were kept warm during the surgical procedure by using a Bair Hugger (3M) to prevent unintended hypothermia. An open midline approach was used for each animal's right knee, followed by a medial parapatellar arthrotomy. The ACL was transected at its tibial and femoral attachments and excised. The surgical site was closed in layers, and a sterile dressing was applied. Animals were housed individually or in pairs in adjacent pens for up to 12 weeks after surgery. The animals were monitored by comparative medicine clinical staff daily for any pain and distress.

Fluid Collection and Biomarker Assessment

The animals were sedated and intubated, and anesthesia was maintained using 1.0% to 3.5% inhaled isoflurane as described earlier for the duration of the specimen collection procedures. Synovial fluid from contralateral uninjured knee samples was collected at baseline (the time of the surgical ACL transection of the injured knee). However, the first collection of synovial fluid from the injured knee was performed at 1 day after injury. Subsequent samples of blood, urine, and synovial fluid for the contralateral uninjured knee and injured knee were then collected at 1, 2, 4, 8, and 12 weeks after injury. Synovial fluid was collected percutaneously from each knee using a sterile technique via a 20-mL syringe and 18-gauge 1.5-inch needle (Becton, Dickinson and Company). The resultant synovial fluid was transferred to a sterile 15-mL tube, aliquoted, and stored at –80°C for future protein analysis. Approximately 16 mL of whole blood was collected percutaneously from the cranial vena cava using a sterile technique at each time point. These blood samples were then centrifuged at 2000g for 15 minutes to isolate serum. Serum was then vortexed, aliquoted into new tubes, and frozen at –80°C. After pigs had recovered from anesthesia, their urine was collected and kept on ice, to be later aliquoted and stored at –80°C.

Quantification of IL-1 β cytokine levels in synovial fluid, serum, and urine was done using a porcine IL-1 beta/IL-1F2 Quantikine ELISA Kit (PLB00B; R&D Systems). To determine the presence of cartilage tissue breakdown in fluid samples, a C-telopeptide of type II

collagen ELISA kit was used (MBS777608; MyBioSource). For IL-1 β and type II collagen assays, samples were allowed to thaw at room temperature and were not diluted when the assays were performed. Standard curves were performed in accordance with the standard values indicated by the manufacturer of the ELISA kits. All data sets were exported to Excel, and concentrations were calculated using interpolation in Prism 8 software (GraphPad).

hBM-MSC Isolation

The Cedars-Sinai Medical Center Institutional Review Board approved this study, and any limited participation of humans was with their informed consent. Donors were enrolled: men and women aged between 30 and 50 years without any malignancy, metabolic disorder, or infectious disease. Isolation of hBM-MSCs was performed as previously described.^{3,36,46} Briefly, hBM was recovered from trabecular bone samples obtained from patients undergoing corrective orthopaedic surgery. The hBM-containing trabecular bone sample was flushed with phosphate-buffered saline. After the whole hBM had been collected, it was centrifuged at 900g for 10 minutes. The pellet was resuspended in 40 mL of phosphate-buffered saline, after which it was layered on lymphocyte separation medium (ICN Pharmaceuticals) and centrifuged at 900g for 30 minutes at 30°C without a break. Mononuclear cells were collected and washed once with phosphate-buffered saline, after which they were recovered by centrifugation for culture expansion. The mononuclear cells were plated in tissue culture dishes at a density of 10–15 $\times 10^6$ cells per 100-mm culture dish at 37°C in 5% CO₂/95% air. The medium was changed after 72 hours and again every 3 to 4 days. Between days 14 and 16, the cells were detached by incubating them with 0.25% trypsin–EDTA for 5 to 10 minutes. The cells were replated at a density of 5 $\times 10^4$ cells/cm² and expanded for 4 passages.

hBM-MSC Labeling With Reporter Gene

hBM-MSCs were transduced with a lentiviral vector harboring Luc under the constitutive ubiquitin promoter to allow for in vivo imaging of cells as previously reported.^{25,27,44,45,49} Stable transfection of hBM-MSCs-Luc and constitutive expression of Luc were validated by performing quantitative bioluminescence imaging over 6 passages as previously described.⁴⁹ No significant change ($P > .05$) in Luc expression was found in subsequent passages, indicating that bioluminescence imaging could be used to track hBM-MSCs-Luc in vivo.

FH(ICG) Synthesis, Cell Labeling, and Preparation for Implantation

The cells were then labeled with FDA-approved FH nanoparticles combined with ICG. This FH(ICG) combined molecule was shown to be detectable using fluorescence and MRI without affecting a cell's biological properties.³¹ FH(ICG) was prepared using a previously published mixing method.⁴⁰ Briefly, FH was purchased from AMAG Pharmaceuticals. ICG and phosphate-buffered saline were purchased from Fisher Scientific. Deionized water was prepared using a Milli-Q reverse osmosis system (MilliporeSigma). Briefly, ICG was dissolved in deionized water at 10 mg/mL, and 3 mL of the ICG solution was added to 3 mL of FH (30 mg/mL, iron). The FH(ICG) solution was mixed briefly and then diluted with phosphate-buffered saline to a 10-mg/mL iron concentration. FH(ICG) was stored in the dark at 4°C and used for up to 28 days after initial preparation. MSCs were treated overnight

with FH(ICG) (100 µg/mL, iron). After overnight treatment, cells were washed with phosphate-buffered saline and collected for implantation. Before implantation, the cells were also labeled with the lipophilic membrane dye DiI as previously reported.^{11,36,42,43} For the injection procedure, 10^7 cells were resuspended in 500 µL of fibrin gel (TISSEEL; Baxter Healthcare Corporation) as previously reported.^{36,37,42,45,47,48} Briefly, to slow the gelling process and to allow for an exact amount of cells to be injected, the thrombin solution was diluted 1:1 with sterile normal saline. Fibrinogen solution with resuspended cells was then mixed with the diluted thrombin solution using pipettes immediately before the intra-articular injection procedure. Using a sterile technique, 500 µL of the cells-fibrinogen-thrombin mixture was then loaded into a 1-mL syringe. While the animal was appropriately anesthetized, an 18-gauge needle was used to inject sterile radi-opaque dye into the affected knee joint under fluoroscopic guidance using a separate syringe. After confirmation of appropriate needle placement. The 18-gauge needle was kept in the joint space, and the 1-mL syringe (with cells resuspended in fibrin gel solution) was attached to it, maintaining the sterile technique. This allowed for the percutaneous injection of cells and fibrin gel into porcine knees under fluoroscopic guidance 2 days after the surgically created ACL injury.

Tracking-Injected MSCs

To image the cells using optical imaging, the pigs were euthanized in compliance with the 2019 guidelines of the American Veterinary Medical Association. In brief, while the animal was under general isoflurane gas anesthesia, commercially available euthanasia solution (1 mL per 4.5 kg of body weight) was administered intravenously. Death was confirmed by identifying complete cessation of heartbeat by stethoscope auscultation and/or anesthetic monitoring equipment reading (electrocardiogram, pulse oximeter). The limbs were then harvested via transection at the level of the proximal femur, and intact knee joints were injected with luciferin solution (50 mg in 400 µL) mixed with contrast agent in a 1:1 ratio under fluoroscopic guidance to ensure appropriate delivery of luciferin solution into the joint space. Images were then acquired using the IVIS Spectrum Bioluminescence system (Perkin Elmer) approximately 10 minutes after luciferin injection. Fluorescence imaging was performed using the far-red and red wavelengths to also detect DiI and ICG fluorescent probes, respectively. MRI studies of FH(ICG)-labeled cells within the joint space were also performed.

MRI of Injured and Uninjured Knees

After euthanasia, the injured and contralateral knee joints were harvested via transection at the proximal femur. All knee joints were imaged in a 3-T clinical magnetic resonance scanner (Prisma; Siemens Healthcare) equipped with a dedicated 18-channel knee coil. Pig limbs were oriented in the supine position with the coil centered on the knee. The MRI protocol consisted of localizer, T1-weighted spin echo, and T2-weighted fast spin echo sequences for each knee in the axial, coronal, and sagittal planes per the following parameters: a repetition time of 4000 milliseconds, an effective echo time of 70 milliseconds, and a field of view of 112.5×150 mm with a matrix of 288×384 , yielding an in-plane resolution of $391 \mu\text{m} \times 391 \mu\text{m} \times 3$ -mm slice resolution. Total scan time was approximately 40 minutes for each knee. The resultant images were reviewed by a

fellowship-trained musculoskeletal radiologist who was blinded to the injured and uninjured knees.

Histologic Analysis

Gross and histologic evaluations of the joint cartilage were performed at 4 or 12 weeks after injury, as previously described.^{39,48,52} Briefly, the knee joints of study animals were harvested using an orthopaedic saw and grossly inspected for the percentage of joint surface noted to be pathologic. The samples were then fixed in 4% formalin for 72 hours, decalcified using trichloroacetic acid (TCA) 6% solution for 3 to 4 weeks, dehydrated, and embedded in paraffin. Tissue sections were cut at a thickness of 5 mm and subsequently stained using hematoxylin and eosin and safranin O.⁴⁵ Representative histologic sections were reviewed by a blinded examiner (T.J.K.) and assigned a grade and a stage, which were used to calculate the Osteoarthritis Research Society International (OARSI) score as previously described.³⁹

Statistical Analysis

All statistical analyses were performed using Prism 8 (GraphPad); $P < .05$ was considered statistically significant. The outcome measurements were level of protein expression measured by ELISA, bioluminescence imaging signal, MRI, and histology. To minimize interanimal variability, changes of the normalized results with time within and across experimental groups were analyzed. Two-way analysis of variance was performed separately for each dependent outcome measure using mean values; Tukey post hoc test was used for multiple comparisons. In Figures 1 and 4, results are presented as mean values, and bars indicate standard deviations.

RESULTS

Inflammatory and OA Biomarker Analysis

To monitor the development of the inflammatory milieu after ACL injury, we examined the expression of a major marker of inflammation within the joint space, IL-1 β , in the synovial fluid, serum, and urine. Synovial fluid analysis showed temporary elevation of IL-1 β 1 week after the injury as compared with the contralateral knee; however, by 2 weeks after injury, IL-1 β levels were not significantly different from those of the contralateral knee (Figure 1A). The presence of IL-1 β in the contralateral knee synovial fluid was negligible and did not change throughout this investigation. In the serum, IL-1 β was elevated shortly after the surgery, followed by a downward trend over the first 4 weeks of the study (Figure 1B). However, in the urine, very low levels of IL-1 β were detected in the first 4 weeks after surgery, and these levels tended to increase on week 8. By 12 weeks after surgery, IL-1 β levels in the urine were significantly increased (Figure 1C).

Increasing levels of type II collagen were found in the synovial fluid on weeks 4 and 8 as compared with contralateral knees. In the serum, there was a statistically significant elevation of the detected collagen fragments at 4 weeks after surgery, indicating the slow breakdown of the articular cartilage extracellular matrix during this period (Figure 1E). However, the level of detected type II collagen was decreased toward the end of the

experiment by week 12. This trend was also reflected by the urinary clearance of the type II collagen that was detected during this same period (Figure 1F).

MRI Evaluation of Injured and Uninjured Knees

Upon review of the MRI by a fellowship-trained musculoskeletal radiologist, there were no appreciable cartilage abnormalities identified in any of the knee compartments of our study animals, even at 12 weeks after ACL injury (n = 3 animals, 6 knees in total). This included injured and uninjured knees. A representative MRI scan of an uninjured knee and injured knee is shown in Figure 2.

MSC Tracking Using Optical Imaging and MRI

To explore the feasibility of MSC therapy in this model, we tested if human MSCs can survive and be detected within the porcine knee joint. At 2 days after the ACL transection procedure, hBM-MSCs containing Luc construct cells were injected into the injured knee joint of study animals under fluoroscopic guidance with the addition of an Omnipaque contrast agent (Figure 3A). The reporter gene-labeled cells were detected using bioluminescence imaging immediately after injection of cells (Figure 3B) and at 2 weeks after injection (Figure 3E). The cells were also detected with fluorescence imaging (Figure 3, C and D) and MRI (Figure 3F). The signal from both fluorescent markers (DiI and ICG), bioluminescence imaging (Luc), and MRI (FH) all colocalized with the site of previous intra-articular injection, indicating that these cells were localized well on fluoroscopic guidance and survived within the injured joint space for 2 weeks in vivo.

Gross Anatomy Images and Histologic Analysis

Signs of OA formation could be detected as early as 4 weeks after ACL transection and were more profound at 12 weeks. After 12 weeks, a prominent OA phenotype could be detected upon gross inspection (Figure 4A) and on histology using hematoxylin and eosin (Figure 4B) and safranin O (Figure 4C) stains. OARSI scoring of the tibial and femoral cartilage demonstrated significant differences between the contralateral, uninjured control knees and the injured knees at 12 weeks after injury at the femur and the tibia ($P < .001$) (Figure 4, D and E).

Of note, at 2 weeks after the injection of cells and fibrin gel, there was no appreciable fibrin gel product on gross inspection of the joint via open arthrotomy. In addition, no adverse events were noted at any time point among the animals included in these experiments.

DISCUSSION

The purpose of this study was to characterize a porcine model of PTOA and describe a novel technique for the percutaneous intra-articular delivery of transgenic human MSCs in the setting of a translational porcine model of PTOA after ACL injury. Our results demonstrate that transection of the ACL in porcine knees leads to cartilage degeneration and intra-articular cytokine changes analogous to those observed in human PTOA. Furthermore, we have characterized the early biomarker profiles of these changes in synovial fluid, serum, and urine in our porcine model. In addition, we have shown that xenogeneic MSCs are

viable within the injured knee joint for at least 2 weeks after percutaneous implantation and that these viable cells continue to express transgenic proteins.

Other groups have characterized porcine models of PTOA and have shown that the cartilage changes observed in this translational model mimic those observed in human PTOA after ACL injury.^{50,56} Wei et al⁵⁶ demonstrated progressive gross chondral changes and progressive loss of glycosaminoglycan content in the cartilage of injured pigs when followed for 6 weeks after ACL transection. In addition, these cartilage matrix changes correlated well with cartilage signal alterations detected on quantitative dGEMRIC MRI. Sieker et al⁵⁰ noted glycosaminoglycan content changes in the cartilage of porcine knees at 4 weeks after ACL transection. The authors also characterized the molecular changes occurring after ACL injury in their porcine model, noting a multitude of RNA expression changes induced by ACL transection. These RNA expression changes included genes that have a well-established role in the development of human PTOA.⁵⁰ These studies corroborate our findings of progressive glycosaminoglycan content loss in the cartilage matrix of porcine knees after ACL transection (Figure 4C), and as is important in any animal model of human disease, these changes are a known feature of human PTOA.³⁸

Multiple studies have tried to assess the survival of exogenous MSCs in a large animal model. Although in vivo imaging can be easily used to track cells in small animals,^{6,45,49} in vivo imaging in large animals has largely been limited to nanoparticle-labeled MSCs tracked via MRI^{15,27} (Figure 3F). The disadvantage of this labeling system is that the signal will persist even after the cells have died or been phagocytosed by local macrophages.² In our study, we have demonstrated the detection of cells labeled with dyes that integrate into the cell membrane (Figure 3C), which allows for the eventual identification of retained exogenous cells on histology.^{42,43,49} However, these membrane-labeled cells cannot currently be tracked in vivo over time, and the detection of signal from these membrane dyes does not confirm cell viability.⁶ The detection of Luc activity (Figure 3E), however, does demonstrate cell viability while providing localization data. As a result, in this study, to provide in vivo evidence of transgenic cell localization and demonstrate the sustained viability of these cells, we used a combination of in vivo and ex vivo imaging techniques. While we do not suggest this approach as a routine method for longitudinal monitoring of therapeutic exogenous cells, this combination of imaging techniques does demonstrate the feasibility of exogenous MSC survival and transgene expression within the joint environment for at least 2 weeks after percutaneous implantation.

Numerous other investigators have reported their results with regard to the intra-articular delivery of MSCs in the treatment of OA, PTOA, or cartilage defects in large and small animal models as well as in human clinical trials; however, the majority of these studies have evaluated only the therapeutic effects on cartilage rather than demonstrating survival of these intra-articularly injected cells.^{22,29,30,53,55,59} Furthermore, most of the injected MSCs in these studies were naïve MSCs or induced toward a chondrogenic fate rather than being transgenic cells. Similar to our study, Khatab et al²² investigated the effect of intra-articular delivery of human MSCs in an immunocompetent murine model of OA. Although the authors did not evaluate the survival of these human MSCs within the joint space, they were able to demonstrate reduced pain and decreased cartilage damage among animals treated

with human MSCs as compared with controls. Yang et al⁵⁸ characterized the biodistribution and distant major organ effects (ie, an assessment of toxicity and off-target effects) of murine MSCs delivered intra-articularly using a murine model of rotator cuff tear. Although the therapeutic cells in this study were not xenogeneic or transgenic cells and the intra-articular delivery of therapeutic cells in the setting of a supraspinatus repair is quite different than that in a knee joint (which has undergone a multilayered closure after arthroscopy), Yang et al did provide evidence that therapeutic MSCs can be cleared in vivo via the renal and gastrointestinal systems and that these cells exhibit no apparent inflammatory effects or toxicity on distant major organs. While the authors were able to detect these labeled cells in vivo for up to 4 weeks after implantation, the biocompatible quantum dot-labeling approach used in this study does not necessarily reflect living cells. Unfortunately, resident macrophages can harbor these exogenous metallic nanoparticle markers after phagocytosis of nanoparticle-labeled apoptotic cells.²⁷ To our knowledge, our study is the first to demonstrate the intra-articular survival and transgene expression of human cells in a large animal model. As a result, this model constitutes an excellent approach for translational investigations of therapeutic MSCs in the setting of PTOA after ACL injury.

Animal models of PTOA demonstrate that the inflammatory cascade plays a critical role in the development of articular cartilage degradation.^{16,17,32} This cascade is mediated by inflammatory cytokines that activate catabolic biologic agents. Previous studies detected matrix metalloproteases and interleukins as major players that mediate this process within the knee joint.^{20,32,51} In this study, we chose to measure IL-1 levels because IL-1 is thought to be a major component of the inflammatory cascade and subsequent catabolic response within the joint space after ACL injury. IL-1 alpha (IL-1 α) has been shown to decrease chondrocyte viability and proliferation in vitro.⁴¹ Furthermore, overexpression of IL-1 β alone has been shown to induce joint degradation in vivo,¹⁶ whereas intra-articular delivery of soluble IL-1 β receptor molecules, acting as a competitive inhibitor of IL-1, can significantly reduce cartilage matrix degradation in animal models of arthritis.¹⁷ Irie et al²¹ reported IL-1 β levels rising abruptly in the human knee after ACL injury and then returning to baseline levels approximately 1 week after injury. This is concordant with the data in our porcine model, which showed an almost immediate response and peak of IL-1 β in the knee joint after ACL injury, followed by resolution of this IL-1 elevation by 1 to 2 weeks after injury (see Figure 1A). Catterall et al⁹ observed that IL-1 β protein levels in human knee synovial fluid were much higher than IL-1 β levels in the serum after ACL injury. In addition, these authors reported an increase in type II collagen levels in the synovial fluid of human knees between about 2 and 8 weeks after ACL injury.⁹ These findings corroborate our results, where mean IL-1 β levels were >10-fold higher in the synovial fluid as compared with serum after ACL injury in our study animals and where intra-articular type II collagen levels also increased in these animals between 2 and 8 weeks after ACL injury. This recapitulation of the intra-articular cytokine and biomarker profile changes observed in humans after ACL injury provides evidence in support of this porcine model as being a robust animal model of human acute ACL injury.

In this study, we observed that IL-1 levels in the urine increased at 8 and 12 weeks after injury. One explanation for this is the high likelihood of ongoing instability. The increased posterior slope of the porcine tibial plateau combined with ACL insufficiency presumably

leads to recurrent instability, as the animals participate in various activities, such as running, walking, and interacting with caregivers throughout the course of this study. Thus, there will be acute mechanical joint injuries and the associated biologic responses occurring over a background of chronic biologic changes in response to the index injury. As a result, it is assumed that these elevated IL-1 levels at weeks 8 and 12 after injury are due to recurrent instability episodes also known as acute on chronic disease.

Standard magnetic resonance sequences obtained in our study using a clinical-grade 3-T machine demonstrated no significant cartilage signal intensity alterations up to 12 weeks after ACL injury. It should be noted that this observation is consistent with clinical findings in humans, where there are also typically no detectible magnetic resonance signal intensity changes noted in the knee cartilage of humans with ACL injury even a few years after the initial injury. This observation is likely due to a lack of sensitivity of current standard clinical MRI sequences reflecting an inability to detect minor cartilage abnormalities that are clinically occult. Although others have reported an ability to detect early cartilage matrix changes in a porcine model after ACL injury,⁵⁶ these studies used highly specialized quantitative MRI techniques, such as dGEMRIC. Unfortunately, given the FDA black box warning on gadolinium contrast agents and the limited availability of clinical magnetic resonance arthrogram resources, these specialized image acquisition techniques are not particularly practical in the clinical setting at this time. Thus, future studies of more specialized cartilage-sensitive sequences, such as T1 ρ ,^{19,57} will likely be an important next step in our ability to noninvasively evaluate early cartilage injury in humans.

One feature that distinguishes our study from other studies of PTOA after ACL injury is our observation that transgenic human MSCs can be detected in the porcine knee up to 2 weeks after percutaneous implantation, as evidenced via intra-articular localization of labeled cells using optical imaging and MRI. Survival of these cells is confirmed by the detection of bioluminescence that reflects the active expression of Luc reporter gene. This finding demonstrates excellent therapeutic potential for several reasons. The survival of MSCs after percutaneous injection into the joint in combination with clinical-grade fibrin glue demonstrates significant translational prospects. Fibrin glue is currently readily available for human applications and has a strong track record of being successfully applied clinically to support cell-based therapies within the human knee joint.^{8,12,13} Fibrin glue is the recommended product used to facilitate matrix-induced autologous chondrocyte implantation, a cartilage restoration therapy approved by the FDA for use in humans. In addition, the ability to use human cells rather than nonhuman cells for efficacy experiments in this porcine model increases the translational potential of this approach. If we can optimize the therapeutic efficacy of these human cells expressing therapeutic transgenic proteins, effectively using these cells as transient drug delivery tools, this will greatly facilitate the progression of this approach along the late translational pathway toward clinical trials. Furthermore, the timing of altered cytokine levels (eg, IL-1 β) in the human knee joint after ACL injury coincides well with the duration of our observed exogenous MSC survival in the porcine knee joint. Specifically, IL-1 β protein levels in the synovial fluid of the human knee have been shown to rise and then normalize over a duration of approximately 2 weeks.²¹ The exogenous MSCs in our study exhibited transgene expression at 2 weeks after implantation. Thus, our model provides an excellent approach to evaluate

potential therapies utilizing transient expression (including expression induced via nonviral mechanisms) of a therapeutic transgene in a translationally relevant large animal model. Finally, the survival of xenogeneic MSCs in the joint space of an immunocompetent large animal in our model indicates that human MSCs likely have immunomodulatory properties, which implies that allogenic human MSCs may be a viable “off the shelf” clinical treatment approach to treating these injuries in humans in the future (ie, allogenic human MSCs may also be able to avoid an immune response within the human knee).

This study does raises questions regarding the mechanism by which human cells remain viable within a porcine host. One explanation for how xenogeneic cells could survive within the intra-articular environment is that the joint space is relatively immunologically privileged. However, if this is the case, in our model, the joint has experienced an injury, and as a result, the joint environment is enriched with inflammatory cells. Therefore, a more likely explanation is based on evidence to suggest that MSCs secrete biologic factors that allow these cells to avoid immune surveillance.^{1,4,6}

Also noteworthy is the fact that pilot experiments where hBM-MSCs-Luc were injected into the knee joint space without fibrin gel did not result in the detection bioluminescence or fluorescence signals *ex vivo*. Possible explanations for this include a lack of cell survival related to a lack of requisite adhesion molecule or cytoskeletal signaling (ie, some form of mechanotransduction) or the inability of our imaging approach to detect cell densities below a certain threshold (ie, cells dispersed throughout the joint do not generate sufficient bioluminescence or fluorescence signal in comparison with clustered cells). We previously used the fibrin gel for cell delivery and to prevent the cells from disseminating diffusely.^{36,42,45,47,48} Although in this study we did not expect the cells to differentiate into a specific tissue type or regenerate any tissue defects, their localization within a particular region of the joint may contribute to their survival and our ability to follow their viability using bioluminescent imaging.

By combining *in vivo* and *ex vivo* imaging with the quantification of bodily fluid biomarkers in this porcine model, we have provided a more comprehensive perspective on the *in vivo* biologic alterations associated with ACL injuries. The majority of *in vivo* studies of ACL injury report on the expression of inflammatory markers only within the synovial fluid,^{20,32,51} whereas in our study we have combined the synovial fluid analysis with an analysis of systemic biomarkers in the serum and the urine. As a result, our findings reflect the quantification of these secreted factors in the serum as well as their subsequent clearance in the urine, and this may provide insight into future clinical studies aimed at noninvasively (ie, without performing an arthrocentesis procedure) assessing the metabolic state of an injured joint.

This study does have some noteworthy limitations, many of which are inherent to animal models of human disease. First, this is a study of quadrupeds rather than bipedal humans. In addition, the number of animals in this model is relatively low. Given that we are just demonstrating feasibility in this large animal model, this is a minor weakness. The study period was only 12 weeks, and degenerative changes would certainly progress beyond this time frame; thus, the data included here are merely a representative sample of the

progression of disease in PTOA after ACL injury. The increased posterior slope of the porcine knee and lack of ACL reconstruction being performed in our study animals lead to persistent knee joint instability that may not reflect the natural history of human ACL injury, where the tibial slope is more horizontal and ACL reconstruction is often performed. Despite this, Sieker et al⁵⁰ found that, in their porcine model of ACL injury, RNA expression changes in the cartilage were not significantly different regardless of whether ACL reconstruction was performed or not.

In conclusion, this study demonstrates the feasibility of reproducing the joint degenerative changes, intra-articular cytokine alterations, and body fluid biomarker findings consistent with PTOA after ACL injury in a porcine animal model. Furthermore, we have demonstrated the ability of human MSCs to survive and express a transgene within the knee joint of porcine hosts without immunosuppression. As a result, this model holds great potential to significantly contribute to investigations focused on the development of cell-based therapies in the future.

ACKNOWLEDGMENT

The authors acknowledge Joseph Giaconi, MD for MRI interpretations; the Cedars-Sinai Biomedical Imaging Core for its help with the MRI studies, the Biobank and Translational Research Core for its help with the histology and scanning of the slides, and Samuel Fuchs for creating the images for Appendix Figure A1 (available online).

source of funding:

This study was supported in part by the National Institutes of Health / National Institute of Arthritis and Musculoskeletal and Skin Diseases (K01AR071512) to D.S. This study also received sponsorship from the Cedars-Sinai Medical Center Department of Orthopedics. T.J.K. has received consulting fees from Heron Therapeutics and hospitality payments from Fidia Pharma, Smith & Nephew, and RTI Surgical. AOSSM checks author disclosures against the Open Payments Database (OPD). AOSSM has not conducted an independent investigation on the OPD and disclaims any liability or responsibility relating thereto.

REFERENCES

1. Aggarwal S, Pittenger MF. Human mesenchymal stem cells modulate allogeneic immune cell responses. *Blood*. 2005;105(4):1815–1822. [PubMed: 15494428]
2. Amsalem Y, Mardor Y, Feinberg MS, et al. Iron-oxide labeling and outcome of transplanted mesenchymal stem cells in the infarcted myocardium. *Circulation*. 2007;116(11)(suppl):I38–I45. [PubMed: 17846324]
3. Aslan H, Zilberman Y, Arbeli V, et al. Nucleofection-based ex vivo nonviral gene delivery to human stem cells as a platform for tissue regeneration. *Tissue Eng*. 2006;12(4):877–889. [PubMed: 16674300]
4. Augello A, Tasso R, Negrini SM, et al. Bone marrow mesenchymal progenitor cells inhibit lymphocyte proliferation by activation of the programmed death 1 pathway. *Eur J Immunol*. 2005;35(5):1482–1490. [PubMed: 15827960]
5. Bascunan AL, Biedrzycki A, Banks SA, Lewis DD, Kim SE. Large animal models for anterior cruciate ligament research. *Front Vet Sci*. 2019;6:292. [PubMed: 31555675]
6. Berglund AK, Fortier LA, Antczak DF, Schnabel LV. Immunoprivileged no more: measuring the immunogenicity of allogeneic adult mesenchymal stem cells. *Stem Cell Res Ther*. 2017;8(1):288. [PubMed: 29273086]
7. Bigoni M, Sacerdote P, Turati M, et al. Acute and late changes in intraarticular cytokine levels following anterior cruciate ligament injury. *J Orthop Res*. 2013;31(2):315–321. [PubMed: 22886741]

8. Brittberg M, Recker D, Ilgenfritz J, Saris DBF, SUMMIT Extension Study Group. Matrix-applied characterized autologous cultured chondrocytes versus microfracture: five-year follow-up of a prospective randomized trial. *Am J Sports Med.* 2018;46(6):1343–1351. [PubMed: 29565642]
9. Catterall JB, Stabler TV, Flannery CR, Kraus VB. Changes in serum and synovial fluid biomarkers after acute injury (NCT00332254). *Arthritis Res Ther.* 2010;12(6):R229. [PubMed: 21194441]
10. Chu CR, Szczodry M, Bruno S. Animal models for cartilage regeneration and repair. *Tissue Eng Part B Rev.* 2010;16(1):105–115. [PubMed: 19831641]
11. Cohn Yakubovich D, Sheyn D, Bez M, et al. Systemic administration of mesenchymal stem cells combined with parathyroid hormone therapy synergistically regenerates multiple rib fractures. *Stem Cell Res Ther.* 2017;8(1):51. [PubMed: 28279202]
12. Ebert JR, Fallon M, Ackland TR, Janes GC, Wood DJ. Minimum 10-year clinical and radiological outcomes of a randomized controlled trial evaluating 2 different approaches to full weightbearing after matrix-induced autologous chondrocyte implantation. *Am J Sports Med.* 2020;48(1):133–142. [PubMed: 31765228]
13. Ebert JR, Robertson WB, Lloyd DG, Zheng MH, Wood DJ, Ackland T. Traditional vs accelerated approaches to post-operative rehabilitation following matrix-induced autologous chondrocyte implantation (MACI): comparison of clinical, biomechanical and radiographic outcomes. *Osteoarthritis Cartilage.* 2008;16(10):1131–1140. [PubMed: 18434214]
14. Friel NA, Chu CR. The role of ACL injury in the development of posttraumatic knee osteoarthritis. *Clin Sports Med.* 2013;32(1):1–12. [PubMed: 23177457]
15. Geburek F, Mundle K, Conrad S, et al. Tracking of autologous adipose tissue-derived mesenchymal stromal cells with in vivo magnetic resonance imaging and histology after intralesional treatment of artificial equine tendon lesions—a pilot study. *Stem Cell Res Ther.* 2016;7:21. [PubMed: 26830812]
16. Ghivizzani SC, Kang R, Georgescu HI, et al. Constitutive intra-articular expression of human IL-1 beta following gene transfer to rabbit synovium produces all major pathologies of human rheumatoid arthritis. *J Immunol.* 1997;159(7):3604–3612. [PubMed: 9317160]
17. Ghivizzani SC, Lechman ER, Kang R, et al. Direct adenovirus-mediated gene transfer of interleukin 1 and tumor necrosis factor alpha soluble receptors to rabbit knees with experimental arthritis has local and distal anti-arthritic effects. *Proc Natl Acad Sci U S A.* 1998;95(8):4613–4618. [PubMed: 9539786]
18. Griffin LY, Albohm MJ, Arendt EA, et al. Understanding and preventing noncontact anterior cruciate ligament injuries: a review of the Hunt Valley II meeting, January 2005. *Am J Sports Med.* 2006;34(9):1512–1532. [PubMed: 16905673]
19. Gupta R, Virayavanich W, Kuo D, et al. MR T(1)rho quantification of cartilage focal lesions in acutely injured knees: correlation with arthroscopic evaluation. *Magn Reson Imaging.* 2014;32(10):1290–1296. [PubMed: 25111625]
20. Han PF, Wei L, Duan ZQ, et al. Contribution of IL-1beta, 6 and TNF-alpha to the form of post-traumatic osteoarthritis induced by “idealized” anterior cruciate ligament reconstruction in a porcine model. *Int Immunopharmacol.* 2018;65:212–220. [PubMed: 30317108]
21. Irie K, Uchiyama E, Iwaso H. Intraarticular inflammatory cytokines in acute anterior cruciate ligament injured knee. *Knee.* 2003;10(1):93–96. [PubMed: 12649034]
22. Khatab S, van Osch GJ, Kops N, et al. Mesenchymal stem cell secretome reduces pain and prevents cartilage damage in a murine osteoarthritis model. *Eur Cell Mater.* 2018;36:218–230. [PubMed: 30398288]
23. Kiapour AM, Shalvoy MR, Murray MM, Fleming BC. Validation of porcine knee as a sex-specific model to study human anterior cruciate ligament disorders. *Clin Orthop Relat Res.* 2015;473(2):639–650. [PubMed: 25269532]
24. Kilkenny C, Browne WJ, Cuthill IC, Emerson M, Altman DG. Improving bioscience research reporting: the ARRIVE guidelines for reporting animal research. *PLoS Biol.* 2010;8(6):e1000412. [PubMed: 20613859]
25. Kimelman NB, Kallai I, Sheyn D, et al. Real-time bioluminescence functional imaging for monitoring tissue formation and regeneration. *Methods Mol Biol.* 2013;1048:181–193. [PubMed: 23929106]

26. Kraus VB, Birmingham J, Stabler TV, et al. Effects of intraarticular IL1-Ra for acute anterior cruciate ligament knee injury: a randomized controlled pilot trial (NCT00332254). *Osteoarthritis Cartilage*. 2012;20(4):271–278. [PubMed: 22273632]
27. Kremen TJ, Bez M, Sheyn D, et al. In vivo imaging of exogenous progenitor cells in tendon regeneration via superparamagnetic iron oxide particles. *Am J Sports Med*. 2019;47(11):2737–2744. [PubMed: 31336056]
28. Lawrence JT, Birmingham J, Toth AP. Emerging ideas: prevention of posttraumatic arthritis through interleukin-1 and tumor necrosis factor-alpha inhibition. *Clin Orthop Relat Res*. 2011;469(12):3522–3526. [PubMed: 21161742]
29. Lee KB, Hui JH, Song IC, Ardany L, Lee EH. Injectable mesenchymal stem cell therapy for large cartilage defects—a porcine model. *Stem Cells*. 2007;25(11):2964–2971. [PubMed: 17656639]
30. Lee WS, Kim HJ, Kim KI, Kim GB, Jin W. Intra-articular injection of autologous adipose tissue-derived mesenchymal stem cells for the treatment of knee osteoarthritis: a phase IIb, randomized, placebo-controlled clinical trial. *Stem Cells Transl Med*. 2019;8(6):504–511. [PubMed: 30835956]
31. Li K, Chan CT, Nejadnik H, et al. Ferumoxytol-based dual-modality imaging probe for detection of stem cell transplant rejection. *Nanotheranostics*. 2018;2(4):306–319. [PubMed: 29977742]
32. Lieberthal J, Sambamurthy N, Scanzello CR. Inflammation in joint injury and post-traumatic osteoarthritis. *Osteoarthritis Cartilage*. 2015;23(11):1825–1834. [PubMed: 26521728]
33. Lohmander LS, Englund PM, Dahl LL, Roos EM. The long-term consequence of anterior cruciate ligament and meniscus injuries: osteoarthritis. *Am J Sports Med*. 2007;35(10):1756–1769. [PubMed: 17761605]
34. Lohmander LS, Ostenberg A, Englund M, Roos H. High prevalence of knee osteoarthritis, pain, and functional limitations in female soccer players twelve years after anterior cruciate ligament injury. *Arthritis Rheum*. 2004;50(10):3145–3152. [PubMed: 15476248]
35. Mather RC 3rd, Koenig L, Kocher MS, et al. Societal and economic impact of anterior cruciate ligament tears. *J Bone Joint Surg Am*. 2013;95(19):1751–1759. [PubMed: 24088967]
36. Mizrahi O, Sheyn D, Tawackoli W, et al. BMP-6 is more efficient in bone formation than BMP-2 when overexpressed in mesenchymal stem cells. *Gene Ther*. 2013;20(4):370–377. [PubMed: 22717741]
37. Pelled G, Sheyn D, Tawackoli W, et al. BMP6-engineered MSCs induce vertebral bone repair in a pig model: a pilot study. *Stem Cells Int*. 2016;2016:6530624. [PubMed: 26770211]
38. Plaas AH, West LA, Wong-Palms S, Nelson FR. Glycosaminoglycan sulfation in human osteoarthritis: disease-related alterations at the non-reducing termini of chondroitin and dermatan sulfate. *J Biol Chem*. 1998;273(20):12642–12649. [PubMed: 9575226]
39. Pritzker KP, Gay S, Jimenez SA, et al. Osteoarthritis cartilage histopathology: grading and staging. *Osteoarthritis Cartilage*. 2006;14(1):13–29. [PubMed: 16242352]
40. Reichel D, Tripathi M, Butte P, Saouaf R, Perez JM. Tumor-activatable clinical nanoprobe for cancer imaging. *Nanotheranostics*. 2019;3(2):196–211. [PubMed: 31183314]
41. Schuerwegh AJ, Dombrecht EJ, Stevens WJ, Van Offel JF, Bridts CH, De Clerck LS. Influence of pro-inflammatory (IL-1 alpha, IL-6, TNF-alpha, IFN-gamma) and anti-inflammatory (IL-4) cytokines on chondrocyte function. *Osteoarthritis Cartilage*. 2003;11(9):681–687. [PubMed: 12954239]
42. Sheyn D, Ben-David S, Shapiro G, et al. Human induced pluripotent stem cells differentiate into functional mesenchymal stem cells and repair bone defects. *Stem Cells Transl Med*. 2016;5(11):1447–1460. [PubMed: 27400789]
43. Sheyn D, Ben-David S, Tawackoli W, et al. Human iPSCs can be differentiated into notochordal cells that reduce intervertebral disc degeneration in a porcine model. *Theranostics*. 2019;9(25):7506–7524. [PubMed: 31695783]
44. Sheyn D, Cohn-Yakubovich D, Ben-David S, et al. Bone-chip system to monitor osteogenic differentiation using optical imaging. *Microfluidics Nanofluidics*. 2019;23(8):99. [PubMed: 32296299]
45. Sheyn D, Kallai I, Tawackoli W, et al. Gene-modified adult stem cells regenerate vertebral bone defect in a rat model. *Mol Pharm*. 2011;8(5):1592–1601. [PubMed: 21834548]

46. Sheyn D, Pelled G, Netanel D, Domany E, Gazit D. The effect of simulated microgravity on human mesenchymal stem cells cultured in an osteogenic differentiation system: a bioinformatics study. *Tissue Eng Part A*. 2010;16(11):3403–3412. [PubMed: 20807102]
47. Sheyn D, Pelled G, Tawackoli W, et al. Transient overexpression of Ppargamma2 and C/ebpalpha in mesenchymal stem cells induces brown adipose tissue formation. *Regen Med*. 2013;8(3):295–308. [PubMed: 23627824]
48. Sheyn D, Pelled G, Zilberman Y, et al. Nonvirally engineered porcine adipose tissue–derived stem cells: use in posterior spinal fusion. *Stem Cells*. 2008;26(4):1056–1064. [PubMed: 18218819]
49. Sheyn D, Shapiro G, Tawackoli W, et al. PTH induces systemically administered mesenchymal stem cells to migrate to and regenerate spine injuries. *Mol Ther*. 2016;24(2):318–330. [PubMed: 26585691]
50. Sieker JT, Proffen BL, Waller KA, et al. Transcriptional profiling of articular cartilage in a porcine model of early post-traumatic osteoarthritis. *J Orthop Res*. 2018;36(1):318–329. [PubMed: 28671352]
51. Silverstein AM, Stoker AM, Ateshian GA, Bulinski JC, Cook JL, Hung CT. Transient expression of the diseased phenotype of osteoarthritic chondrocytes in engineered cartilage. *J Orthop Res*. 2017;35(4):829–836. [PubMed: 27183499]
52. Turgeman G, Pittman DD, Muller R, et al. Engineered human mesenchymal stem cells: a novel platform for skeletal cell mediated gene therapy. *J Gene Med*. 2001;3(3):240–251. [PubMed: 11437329]
53. Ude CC, Sulaiman SB, Min-Hwei N, et al. Cartilage regeneration by chondrogenic induced adult stem cells in osteoarthritic sheep model. *PLoS One*. 2014;9(6):e98770. [PubMed: 24911365]
54. van Buul GM, Kotek G, Wielopolski PA, et al. Clinically translatable cell tracking and quantification by MRI in cartilage repair using superparamagnetic iron oxides. *PLoS One*. 2011;6(2):e17001. [PubMed: 21373640]
55. Vangsness CT Jr, Farr J 2nd, Boyd J, Dellaero DT, Mills CR, LeRoux-Williams M. Adult human mesenchymal stem cells delivered via intra-articular injection to the knee following partial medial meniscectomy: a randomized, double-blind, controlled study. *J Bone Joint Surg Am*. 2014;96(2):90–98. [PubMed: 24430407]
56. Wei B, Zong M, Yan C, et al. Use of quantitative MRI for the detection of progressive cartilage degeneration in a mini-pig model of osteoarthritis caused by anterior cruciate ligament transection. *J Magn Reson Imaging*. 2015;42(4):1032–1038. [PubMed: 25656460]
57. Witschey WR, Borthakur A, Fenty M, et al. T1rho MRI quantification of arthroscopically confirmed cartilage degeneration. *Magn Reson Med*. 2010;63(5):1376–1382. [PubMed: 20432308]
58. Yang Y, Chen J, Shang X, et al. Visualizing the fate of intra-articular injected mesenchymal stem cells in vivo in the second near-infrared window for the effective treatment of supraspinatus tendon tears. *Adv Sci (Weinh)*. 2019;6(19):1901018. [PubMed: 31592419]
59. Zhang R, Ma J, Han J, Zhang W, Ma J. Mesenchymal stem cell related therapies for cartilage lesions and osteoarthritis. *Am J Transl Res*. 2019;11(10):6275–6289. [PubMed: 31737182]

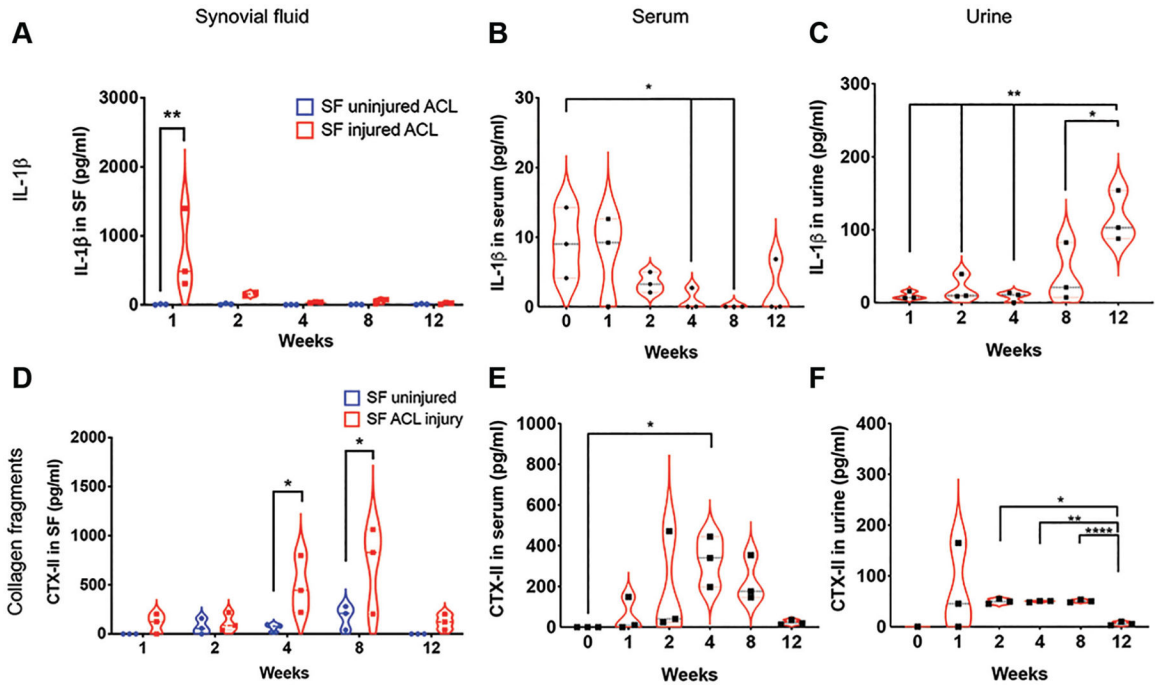


Figure 1.

Elevation of interleukin 1 (IL-1) and collagen type 2 breakdown products after anterior cruciate ligament (ACL) injury in large animal model. Synovial fluid (SF) from both knees and blood and urine samples were collected from pigs at various time points after ACL transection. The levels of IL-1 β were significantly elevated in the first week after surgery in the SF of injured knees and serum. In the urine, IL-1 elevation was detected only at 12 weeks after injury. Cartilage degradation was measured by an assay for type II collagen breakdown products (CTX-II) and found to be elevated between 2 and 8 weeks after injury in all tested fluids, however, levels decreased at week 12. n = 3. * P < .05. ** P < .01. **** P < .0001.



Figure 2. Representative T2-weighted coronal images for (A) an uninjured porcine knee and (B) injured porcine knee (anterior cruciate ligament transection) at 12 weeks after injury. Note that no significant differences in chondromalacia were noted between injured and uninjured knees.

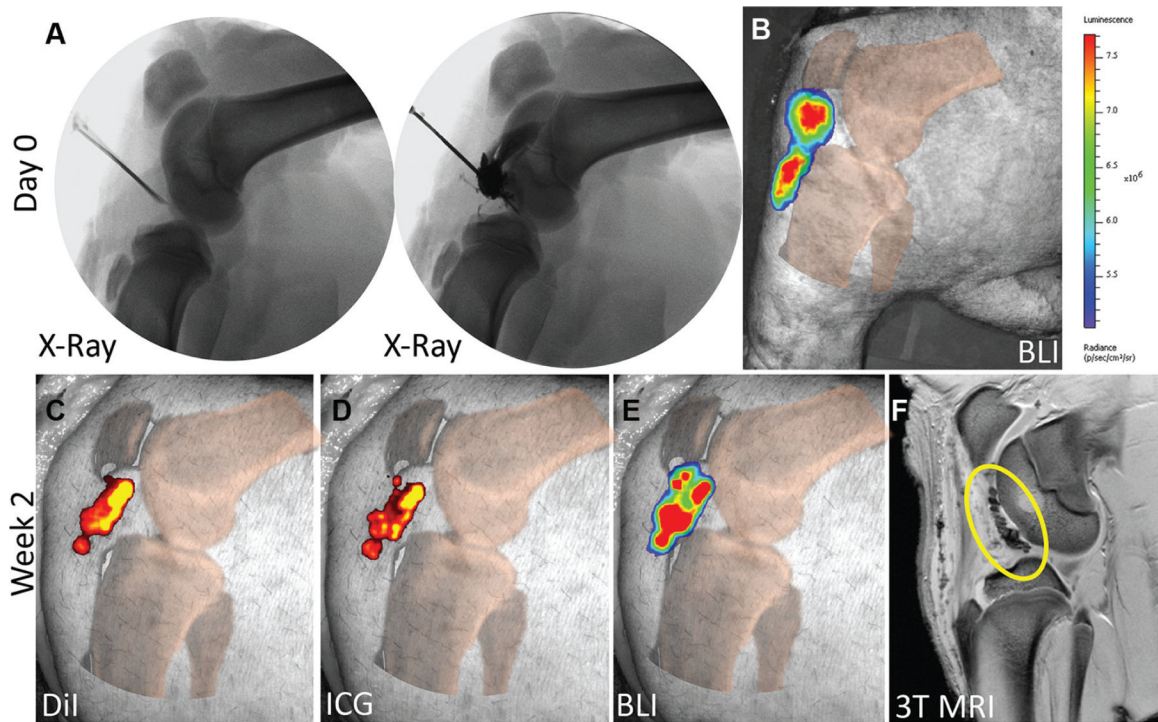


Figure 3.

Intra-articular hBM-MSCs-Luc tracking using bioluminescence imaging (BLI). hBM-MSCs-Luc were prelabeled with DiI fluorescent dye and ICG-loaded Feraheme nanoparticles. (A) hBM-MSCs-Luc mixed with contrast agent were injected into the joint under fluoroscopic guidance. (B) Luciferase activity was visualized using BLI after luciferin injection at day 0. Subsequently, the pigs were sacrificed 2 weeks after injection of cells. Florescent imaging of the (C) DiI-labeled cells and (D) ICG-conjugated Feraheme nanoparticles shows localization of the cells in the knee. (E) BLI signal shows survival of cells in the knee for 2 weeks, and (F) the Feraheme-labeled cells can be detected using MRI (highlighted by yellow region). Images B-E are overlaid with an artificial virtual image of the knee bones for orientation. hBM-MSCs-Luc, human bone marrow–derived mesenchymal stem cells–luciferase reporter gene; ICG, indocyanine green; MRI, magnetic resonance imaging.

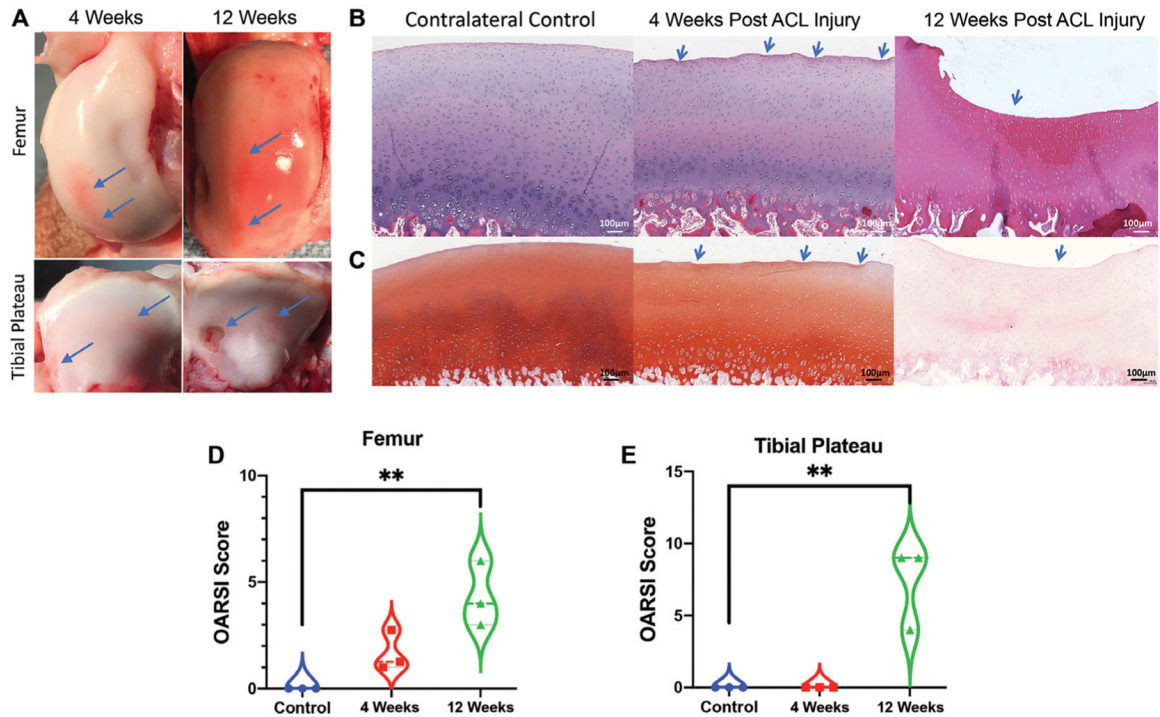


Figure 4.

Gross examination and histologic indications for osteoarthritis formation 4 and 12 weeks after anterior cruciate ligament (ACL) injury in pigs. (A) Macroscopic views of femoral condyles and tibial plateau. Histologic analysis of injured and contralateral uninjured medial femoral condyles: (B) hematoxylin and eosin and (C) safranin O. Chondromalacia with articular surface disruption and fissures at the medial femoral condyles of pigs at 4 and 12 weeks after ACL injury (blue arrows). OARSI scoring of chondral damage at the (D) femur and (E) tibia. OARSI, Osteoarthritis Research Society International. $n = 3$. $**P < .01$.

TABLE 1

Abbreviations

ACL	anterior cruciate ligament
BLI	bioluminescence imaging
FDA	Food and Drug Administration
FH	Feraheme
hBM	human bone marrow
ICG	indocyanine green
IL-1	interleukin 1
Luc	luciferase reporter gene
MRI	magnetic resonance imaging
MSCs	mesenchymal stem cells
OA	osteoarthritis
PTOA	posttraumatic osteoarthritis

Author Manuscript

Author Manuscript

Author Manuscript

Author Manuscript